ACS APPLIED MATERIALS & INTERFACES

Research Article

www.acsami.org

Capture of Tumor Cells on Anti-EpCAM-Functionalized Poly(acrylic acid)-Coated Surfaces

Kiki C. Andree,[*,†,‡] Ana M.C. Barradas,[†,⊥,‡] Ai T. Nguyen,[§] Anouk Mentink,[†] Ivan Stojanovic,[†] Jacob Baggerman,[§] Joost van Dalum,[†] Cees J.M. van Rijn,[∥] and Leon W.M.M. Terstappen[†]

[†]Medical Cell Biophysics Group, MIRA Institute for Biomedical Engineering and Technical Medicine, Faculty of Science and Technology, University of Twente, 7522 NB Enschede, The Netherlands

[§]Aquamarijn Micro Filtration BV, IJsselkade 7, 7201 HB Zutphen, The Netherlands

[∥]Laboratory of Organic Chemistry, Wageningen University, Dreijenplein 8, 6703 HB Wageningen, The Netherlands

Supporting Information

ABSTRACT: The presence of tumor cells in blood is predictive of short survival in several cancers and their isolation and characterization can guide toward the use of more effective treatments. These circulating tumor cells (CTC) are, however, extremely rare and require a technology that is sufficiently sensitive and specific to identify CTC against a background of billions of blood cells. Immunocapture of cells expressing the epithelial cell adhesion molecule (EpCAM) are frequently used to enrich CTC from blood. The choice of bio conjugation strategy and antibody clone is crucial for adequate cell capture but is poorly understood. In this study, we determined the binding affinity constants and epitope binding of the EpCAM antibodies VU1D-9, HO-3, EpAb3-5, and MJ-37 by surface plasmon resonance imaging (SPRi). Glass surfaces were coated using a poly(acrylic acid) based coating and functionalized with anti-EpCAM antibodies. Binding of cells from the breast carcinoma cell line (SKBR-3) to the functionalized surfaces were compared. Although EpAb3-5 displayed the highest binding affinity HO-3 captured the highest amount of cells. Hence we report differences in the performance of the different antibodies and more importantly that the choice of antibody to capture CTC should be based on multiple assays.

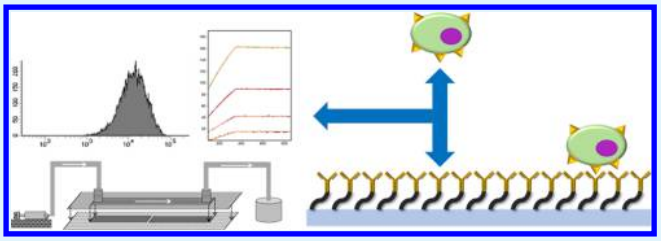

KEYWORDS: *epithelial cell adhesion molecule (EpCAM), antibodies, flow model, polycarboxylate coating, circulating tumor cells, surface plasmon resonance*

INTRODUCTION

Tumor cells present in blood are referred to as circulating tumor cells (CTC) and their load is associated with poor outcome in breast, prostate, lung, and colorectal cancer.[1] The availability of tumor material through a blood sample is generally referred to as a liquid biopsy.[2]

Enumeration and isolation of CTC is challenging as it implies capturing and detecting cells that occur in a frequency of 1 to 10 among billions of blood cells.[3] Capturing strategies can be essentially categorized in those based on differences in physical or immunological properties between CTC and blood cells. Most techniques that explore the immunological properties of CTC target the epithelial cell adhesion molecule CD326 (EpCAM).[4] EpCAM is a type I transmembrane protein and functions as a cell adhesion molecule which is expressed in the majority of normal epithelial tissues but not on blood cells.[5] EpCAM was initially described as a tumor-associated antigen[6] and is of particular interest because it is overexpressed in the majority of human epithelial cancers[7] including colorectal,[8] breast,[9] gastric,[10] prostate[11] and hepatic cancer.[12] Also, it was the first human tumor-associated antigen to be identified with the use of monoclonal antibodies and the first target of monoclonal antibody therapy in humans.[13] The CellSearch system (Veridex, LLC, Raritan, NJ, USA) is the only FDA-cleared system for CTC enumeration and based on CTC enrichment using ferrofluids coated with anti-EpCAM antibodies.[14] Similarly, the CTC-iChip employs magnetic beads coated with anti-EpCAM.[15] Other technologies, such as the Gedi,[16] CTC-Chip,[17] and HB-Chip[18] use anti-EpCAM antibodies functionalized on micropatterned surface of microfluidic devices. Most of the referred technologies use avidin−biotin chemistry as surface functionalization strategy. The choice of anti-EpCAM clone is, however, rarely justified and in some cases not even mentioned. However, this choice can have a dramatic influence in the capture performance of the devices, because the binding affinity to CTC of these antibodies can vary.

Here we report a poly(acrylic acid) coating and functionalization with four different anti-EpCAM antibodies of surfaces to

Received: January 29, 2016
Accepted: May 17, 2016
Published: May 17, 2016

© 2016 American Chemical Society

DOI: 10.1021/acsami.6b01241
ACS Appl. Mater. Interfaces 2016, 8, 14349−14356

capture CTC and compare the ability to capture cells from the breast cancer cell line SKBR-3.

MATERIALS AND METHODS

Materials. Poly(acrylic acid) (PAA) solution, average $M_w \approx$ 250 000, 35% in water; N-(3-(Dimethylamino)propyl)-N′-ethylcarbodiimide hydrochloride (98%, EDC); *N*-hydroxy-succinimide (98%, NHS), MES solution for molecular biology, (0.5 M in water); sodium hydroxide; and absolute ethanol were purchased from Sigma-Aldrich (St.Louis, MO, USA). (3-Aminopropyl)triethoxysilane was purchased from Gelest (Morrisville, PA, USA)

Methods. *Amine-Coated Glass Slides.* Microscope glass slides were cleaned with acetone and wiped with tissues (VWR, Spec-Wipe 3) and subsequently cleaned with piranha solution (1:3, $H_2O_2$3:H_2SO_4) for 30 min to create silanol groups on the surface. The samples were rinsed 3 times with an excess of water. The piranha treated samples were incubated in a solution of (3-aminopropyl)-triethoxysilane (0.1M) in absolute ethanol with water (5%) and acetic acid (0.25%) for 4h at 40 °C. After incubation the samples were rinsed 3 times with ethanol and dried under vacuum.

Poly(acrylic acid) Coating (PAA coating). PAA stock solution was diluted to a concentration of 1 g·L^{-1}. One M NaOH solution was added to the PAA solution to reach a final concentration of 0.005M. EDC (0.006M) and NHS (0.005M) were added into the mixture. After 15 min of stirring, amine-coated glass slides were immersed into the mixture for 1 h under stirring conditions. Subsequently, the samples were rinsed 3 times with excess of water during 1 h. The PAA-coated glass slides were kept at 4 °C until further usage up to 3 weeks after preparation.

Antibody Surface Functionalization. Prior to PAA functionalization, glass slides were dried under a stream of nitrogen. Immediately afterward, slides were placed in a slide holder (Grace Bio-Laboratories ProPlate microarray system) with square 6 × 6 mm^2 microwells. PAA coatings were reacted with a solution of 0.3 M NHS and EDC (NHS/EDC) in MES buffer (100 mM, pH 5.5) at room temperature for 30 min, to obtain a NHS-activated PAA layer. Residual NHS/EDC was washed away with sodium acetate buffer (2 mM, pH 5). All washing steps were carried out in this manner and always repeated 3 times. Anti-EpCAM antibodies or Bovine Serum Albumin (BSA) were pipetted in sodium acetate buffer at a concentration of 20 μg/mL. The following anti-EpCAM clones were used: EpAb3-5[19] (BioMab, Inc., Taipei, Taiwan), HO-3[20] (Trion Research GmbH, Germany) MJ-37[21] (a kind gift of Noel Warner, BD Biosystems, San Jose, CA, USA) and VU1D-9[4] (kind gift from Immunicon, Huntingdon Valley, PA, USA). To capture T-lymphocytes, the anti-CD-3 (clone: UCH-T1, Cat#:ab22, Abcam, Cambridge, UK) was used. Antibodies were permitted to bind for 2 h, after which unbound antibody was washed away. To block any unreacted binding sites, a solution of 0.5 M ethanolamine hydrochloride (E6133, Sigma-Aldrich) in demineralized water was added and incubated for 30 min. After another washing step, the functionalized microscope glass slides were further used for either immunostaining or cell capture experiments.

X-ray Photoelectron Spectroscopy (XPS). The XPS analysis of surfaces was performed using a JPS-9200 Photoelectron Spectrometer (JEOL, Japan). The high-resolution spectra were obtained under UHV conditions using monochromatic Al Kα X-ray radiation at 12 kV and 25 mA, using an analyzer pass energy of 10 eV. High-resolution spectra were corrected with a linear background before fitting.

SKBR-3 Cells. Breast carcinoma cell line SKBR-3 was obtained from ATCC (Manassa, VA, USA) and cultured in DMEM (Gibco, Life Technologies, Waltham, MA, USA) containing 2 mM L-glutamine (G7513, Sigma-Aldrich), 100 U/mL penicillin and 100 μg/mL streptomycin (P4333, Sigma-Aldrich) and 10% FBS (F4135, Sigma-Aldrich). Cells were trypsinized when nearing confluency with 0.05% Trypsin-EDTA (1X) with Phenol Red (Gibco, Life Technologies) and replated at a seeding density never below 20 000 cells/cm^2. Culture medium was refreshed twice a week. Cells were counted using the Luna automated cell counting system (Logos Biosystems, Annandale, VA, USA) by loading 12 μL of cell suspension into the respective counting slides. For dynamic cell capture experiments cells were stained overnight before harvesting using 10 μM Cell Tracker Orange (Invitrogen, Carlsbad, CA, USA). For static cell capture experiments SKBR-3 cells were stained in PBS with 4 μg/mL of Hoechst 33342 (Life Technologies) and used immediately after.

Mononuclear Cells. Blood was collected from healthy (no prior history of cancer or blood transmittable disease) volunteers aged 20−55 who provided informed consent prior to the donation, in accordance to the study protocol approved by the METC Twente ethics committee. Blood was drawn into CellSave vacutainers (Veridex, Raritan, NJ, USA) and processed within 2 h after being drawn using Ficoll-Paque PLUS (GE Healthcare Europe GmbH, Eindhoven, The Netherlands) for mononuclear cell isolation, following the manufacturer's protocol. Mononuclear cells were resuspended in PBS and counted following a similar protocol as described for SKBR-3. Lymphocytes were stained in PBS with 1 μg/mL of Hoechst 33342 (Life Technologies) and used immediately for the cell capture experiments.

Antibody Immunostaining. For secondary antibody immunostaining, sheep antimouse F(ab')2 Anti-Mouse IgG Phycoerythrin (PE) (12−4010−82, eBioscience, San Diego, CA, USA), from here on named anti-IgG-PE, was diluted 40× in PBS, to an approximate concentration between 22.5 and 27.5 μg/mL.

Anti-EpCAM Antibody Cross-Blocking Using Flow Cytometer. Antibody cross-blocking was determined with flow cytometry using a FACSAria II (BD Biosciences, San Jose, CA, USA). Approximately 200,000 SKBR-3 cells were resuspended in PBS after trypsinization. Cells were incubated with each anti-EpCAM antibody (1 μg/mL) followed by incubation with anti-IgG-PE (40× dilution) or VU1D-9-PE (kind gift from Immunicon) (1 μg/mL) for 30 min at Room Temperature (RT) and with Hoechst 33342 (4 μg/mL) for 15 min at 37 °C just before analysis. In between incubation steps, cells were washed with 1% BSA in PBS.

anti-EpCAM Binding Affinity Using Surface Plasmon Resonance Imaging. Antibody binding affinity was measured with SPRi (IBIS MX96, IBIS technologies B.V., Enschede, The Netherlands) using Easy2Spot preactivated G-type Senseye sensors (Ssens BV, Enschede, The Netherlands) as gold SPR sensor surfaces. Recombinant human EpCAM protein (rhEpCAM, Abcam, Cambridge, UK) and the 4 different anti-EpCAM antibodies, previously diluted in 10 mM immobilization buffer (IB) in concentrations ranging from 64 nM to 0.3 nM (obtained in serial dilution factor steps of 3), were immobilized on the sensor surface using the Continuous Flow Microfluidic (CFM) spotter (Wasatch microfluidics LLC, Salt Lake City, Utah, USA).[22] Immobilization buffer (IB) (pH 4.5) was composed of 0.2 M anhydrous sodium acetate solution (Sigma-Aldrich chemie GmbH, Steinheim, Germany), 0.2 M acetic acid solution (Merck Schuchardt OHG, Hohenbrunn, Germany) and ultrapure demineralized water, in the following proportions respectively: 1.93:3.07:95. Sensor areas outside ligand regions (regions of interest) were deactivated with 1% BSA (Sigma-Aldrich chemie GmbH) in IB solution followed by 100 mM ethanolamine solution (MP Biomedicals LLC, Illkrich, France), pH 8. After immobilization and deactivation steps, anti-EpCAM antibodies and rhEpCAM, previously diluted in system buffer (PBS + 0,075% tween), were injected consecutively in concentrations of 32, 16, 8, 4, 2, 1, and 0.5 nM. To obtain kinetic data of the antibody samples, a script was programmed consisting of an initial baseline time of 1 min, followed by 5 min of association between the antibodies and the immobilized ligands and 8 min of dissociation using fresh system buffer, at a flow speed of 4 μL/s. Finally, a regeneration with 10 mM glycine−HCl, pH 2.5, was performed for 1 min, after which the analytes detached from the ligands. Antibody affinity was calculated by the interpolation method for accurate affinity ranking of arrayed ligand—the analyte interactions as described in more detail elsewhere.[23]

Cell Capture Experiments (static and dynamic). For experiments without flow (static conditions), SKBR-3 cells (approximately 30 000 or otherwise if indicated) were pipetted onto the respective microwell. Cells were incubated for 30 min to maximize binding opportunity with surface functionalized proteins (anti-EpCAM or control BSA).

DOI: 10.1021/acsami.6b01241
ACS Appl. Mater. Interfaces 2016, 8, 14349−14356

Scheme 1. Poly(acrylic acid) Grafting to the Glass Surfaces

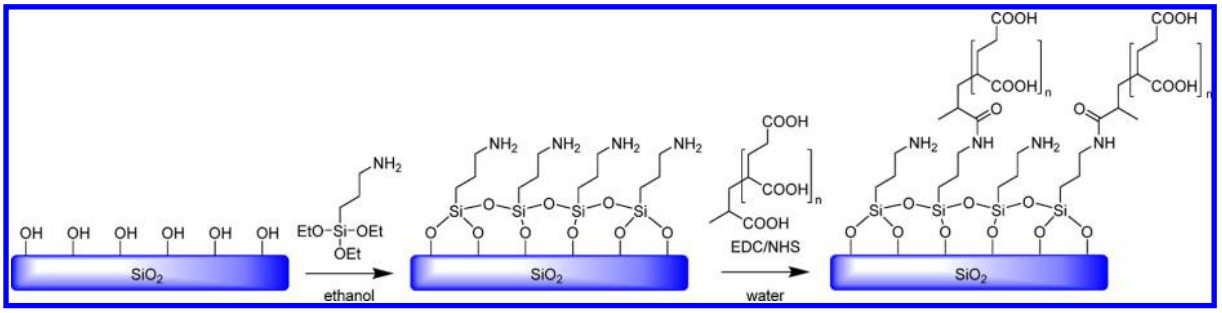

Unbound cells were washed with PBS using a micropipette. The procedure was repeated 3× before microscopy pictures were taken. For experiments under flow (dynamic conditions), the glass slide was released from the holder and immediately after attached to a channel slide 400 μm in height (sticky-Slide I 0.4 Luer, sterile, ibidi GmbH, Munich, Germany). The inlet and outlet ports were connected, with latex rubber tubing, to a syringe filled with the cell suspension and to a waste container. Flow speed was controlled using a syringe pump (NE-1000, ProSense, Oosterhout, The Netherlands). Before applying the cell suspension, the system was primed with clean PBS to remove air bubbles from the tubing and slide channel.

Image Acquisition and Analysis. Images were acquired while maintaining the glass slide in the glass holder (static) or through the channel transparent slide ceiling (dynamic). The microwells area or the slide channel's area were imaged using a fluorescence microscope equipped with a Mercury Arc lamp as light source, a 4× (0.45NA) objective, a computer-controlled CCD camera (Hamamatsu C4742–95–12NRG CCD), a X,Y,Z stage and a 4-filter cube exchanger. The PE filter was used to identify Cell Tracker Orange stained cells. The microscope was controlled with a Labview (National Instruments, Austin, TX, USA) in house-developed script. Before image acquisition, the focal planes were determined using immunofluorescence (*X,Y* plane) and iterative determination of the focus at 16 locations (*Z* plane). All images from one sample were placed in a directory for image analysis. Scanned images from each well were stitched into a whole using the script developed by Preibisch et al.[24] Stitching was required instead of a montage to avoid overlap between adjacent images. For each stitched well, a ROI of 2500 px in diameter was manually selected around the well center, to exclude cells observed at the border of all wells, irrespectively of glass functionalization status. Hoechst stained cells in ROIs were counted with the in house developed CellCounter script executed in Matlab using a non-commercial license of the DIPlib function base. For each experiment, cell counts are the result of 3 averaged wells. In the case of static experiments or secondary immunostaining, images were acquired using a fluorescence microscope (Nikon, Tokyo, Japan) equipped with a 2× and 4× objective (0.45NA), a Hoechst filter and a CCD camera (Hamamatsu C4742-95-12NRG CCD).

Statistical analysis was performed using IBM SPSS statistics, version 23 (IBM, Armonk, NY, USA). Significant difference between cells captured on BSA and EpCAM-functionalized surfaces was calculated using an independent *t* test. A one-way ANOVA using Tukey posthoc multiple comparison was used to determine significant difference between the 4 antibody cell capturing results.

RESULTS

Coating and Antibody Functionalization. Poly(acrylic acid) (PAA) was coated on glass slides to enable covalent binding of antibodies to the surfaces (Scheme 1). This was done by first creating an amine terminated self-assembled monolayer of 3-aminopropyl(triethoxy)silane (APTES) on the surface. To this amine layer PAA was grafted using EDC/NHS chemistry.[25] PAA-coated glass surfaces were characterized by XPS. The wide-scan XPS spectrum showed presence of all expected elements (Supporting Information): carbon from the poly(acrylic acid), carbon and nitrogen from the precursor APTES layer, silicon from glass substrate and oxygen derived from both organic layer and substrate (Figure S1). The narrow-scan XPS spectrum of C_{1s} region of the PAA-coated surface is similar to the published reference XPS data for pure PAA (Figure S2).[26] The results confirmed the presence of PAA on the glass substrate.

After characterization of the PAA coating, an antibody functionalization protocol was developed, based on NHS/EDC chemistry. To prove that the functionalization protocol could immobilize antibodies on the surface exposing active binding sites, we tested the capture of mononuclear cells with anti-CD3 functionalized microscope glass slides. Therefore, glass surfaces were coated as previously described and microwells were created with a microscope glass slide holder and each microwell surface was functionalized with either BSA or anti-CD3. The presence of anti-CD3 was detected using an anti-IgG1-PE. No fluorescence signal from the BSA surface was detected whereas clear fluorescence signals were detected using the CD3 functionalized surface (Figure 1A, B). Next, approximately 50 000 mononuclear cells isolated from blood were stained with Hoechst and added to the functionalized microwells with a micropipette. Cells were incubated for 30 min. After washing with PBS, few lymphocytes remained at the BSA surface (C), whereas many cells were bound to the anti-CD3 surface (D),

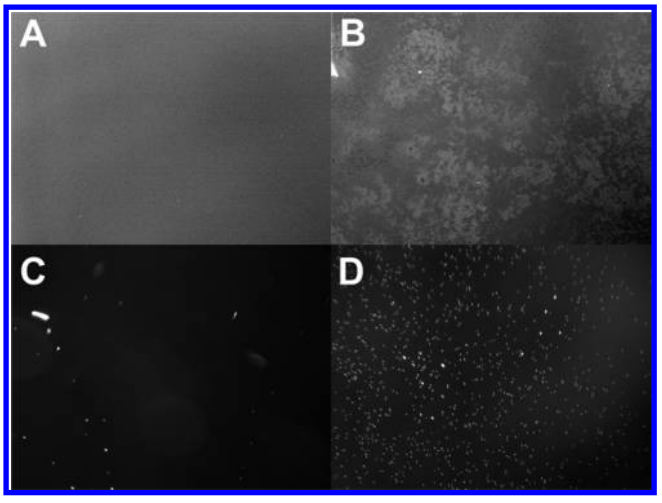

Figure 1. Anti-IgG1-PE staining of a (A) BSA- and (B) CD3-coated microwell region. Mononuclear cells freshly isolated from blood were incubated for 30 min on a (C) BSA-coated and (D) CD3-functionalized surface. After washing, only T-lymphocytes remained bound to the CD3 antibodies compared to the BSA surface.

DOI: 10.1021/acsami.6b01241
ACS Appl. Mater. Interfaces 2016, 8, 14349–14356

indicating that the developed protocol functionalizes the surface with antibodies having exposed active binding sites.

Static and Dynamic Capture of SKBR-3 Cells. Next, we applied the functionalization protocol to VU1D-9, a widely used anti-EpCAM antibody.[27] Capture properties of VU1D-9 functionalized surfaces were tested under static conditions (no flow) using SKBR-3 cells, a well characterized breast carcinoma cell line, known to express high levels of EpCAM.[4] For both static and dynamic experiments, fresh cells were used. Immediately after trypsinization, SKBR-3 cells suspended in PBS were stained with Hoechst. Approximately 30 000 cells were pipetted into microwells coated with VU1D9 and microwells coated with BSA (3 replicates of each condition) and incubated for 30 min, Nonbound cells were removed by washing 3 times with PBS, using a micropipette. Immediately after washing, cells were visualized with a fluorescent microscope and imaged. Figure 2 is a representative image of

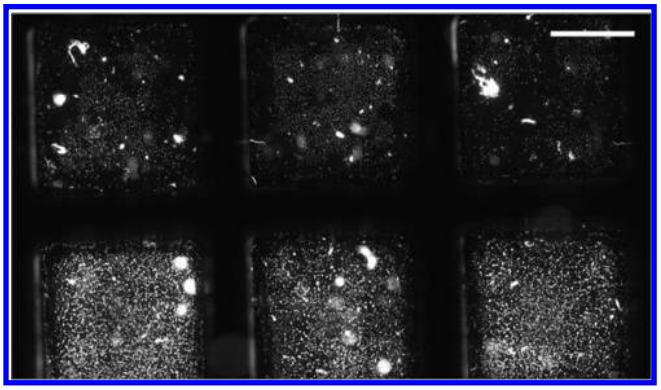

Figure 2. Hoechst stained SKBR-3 cells were allowed to bind for 30 min to BSA (top) or VU1D-9 (bottom) functionalized surfaces. Image is representative of one independent experiment, showing 3 wells per condition. After rinsing the cells 3 times with PBS, SKBR-3 bound 2 times more to the VU1D-9 functionalized microwells than to the BSA wells. Scale bar represents 3 mm.

one of those experiments showing that SKBR-3 cells bound more to the anti-EpCAM functionalized surface than to the control surface. Table 1 summarizes the cells bound by quantification of 2 static independent experiments, showing that SKBR-3 cells bound, on average, 2 times more to the VU1D-9 surface than to the BSA one. These data shows that SKBR-3 cells are specifically captured by an anti-EpCAM-functionalized surface.

Following the static experiments, we developed a model to test SKBR-3 cell capture followed by dynamic washing conditions using flow. For this, we coupled a syringe to a channel slide with a height of 400 μm, and attached onto the prefunctionalized microscope glass slides. Scheme 2 represents the flow model.

Scheme 2. Representation of the Flow Model Used to Test SKBR-3 Cells Capture on BSA and VU1D-9 Antibody-Functionalized Surfaces

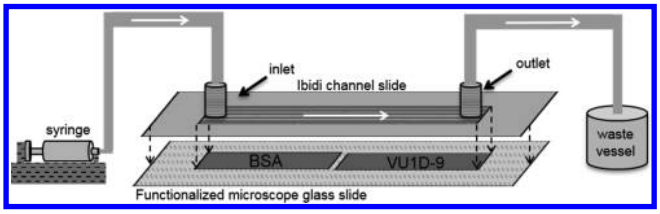

Initially, 600 000 SKBR-3 cells suspended in PBS were added via the syringe reservoir and left to sediment in the channel for 30 min. Following the sedimentation phase, the syringe reservoir was exchanged for PBS and the flow switched on at 100 μL/min and maintained for 30 min. After that period, the flow was set to 500 μL/min for another 30 min. Figure 3 shows

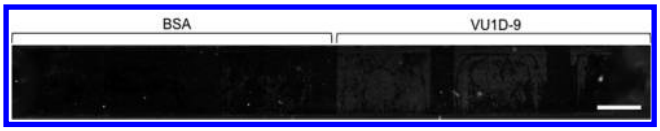

Figure 3. Hoechst stained SKBR3 cells were allowed to flow for 30 min through BSA (control) and VU1D-9 functionalized surfaces. Image is representative of one independent experiment. SKBR-3 bound approximately 3−4 times more to the VU1D-9-functionalized glass surface than to the BSA one. Scale bar represents 3 mm.

that more cells bound to the VU1D-9-functionalized surface than to the BSA surface, indicating that also under dynamic conditions the epitope-antibody binding is sustained. Quantification of cell numbers described in Table 1 for two independent dynamic experiments shows that of all bound cells, 78 and 85% of the cells bound to the VU1D-9 surface.

Antibody Affinity and Cross-Blocking. To test whether the PAA coating could be functionalized with various anti-EpCAM antibodies, we applied the same functionalization protocol to four different antibodies and performed a secondary immunostaining to detect their presence.

Microwells were defined in a microscope glass slide following functionalization. In each microwell, the glass slide surface was functionalized with one of the following antibodies: EpAb3-5, HO-3, MJ-37 and VU1D-9, the most widely used anti-EpCAM antibodies for CTC applications. In addition, a BSA-functionalized surface and an empty one (same functionalization protocol except that protein incubation step was performed only with the buffer) were used as controls. After functionalization, the surfaces were incubated with an Anti-IgG-PE antibody and visualized with a fluorescence microscope.

There was no fluorescent signal coming from the BSA and empty surfaces (Figure 4 A and B) whereas signal could be detected in all surfaces functionalized with the anti-EpCAM

Table 1. Quantification of SKBR3 Cells Bound to BSA and VU1D9 Functionalized Surfaces under Static and Dynamic Conditions

	experiment	BSA-bound cells[a]	VU1D-9-bound cells[a]	percentage BSA bound	percentage VU1D-9 bound	p value[b]
static	1	626	1264	33%	67%	0.08
	2	1164	2379	33%	67%	0.005
dynamic	1	1107	3877	22%	78%	0.03
	2	1923	11318	15%	85%	0.03

[a]Average of 3 wells. [b]p value calculated with a Student's t test.

DOI: 10.1021/acsami.6b01241
ACS Appl. Mater. Interfaces 2016, 8, 14349−14356

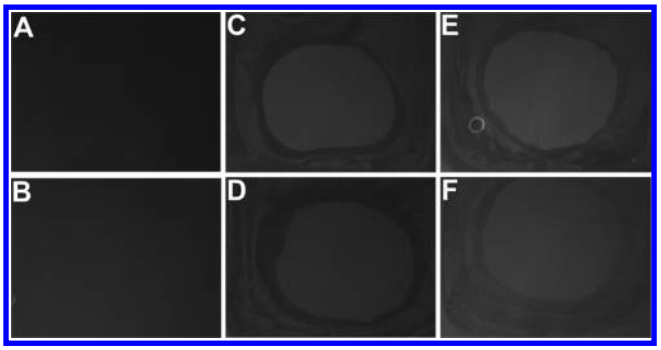

Figure 4. Anti-IgG-PE staining of a blank glass microscope slide surface (A), treated as described in the functionalization protocol except that protein incubation was performed with sodium acetate buffer only, and of functionalized surfaces with BSA (B), VU1D-9 (C), HO-3 (D), EpAb3-5 (E) and MJ-37 (F). Only anti-EpCAM functionalized surfaces stained positive.

antibodies (Figure 4, C–F), indicating that the functionalization protocol can be applied to several antibodies.

Flowcytometry was used to determine cross blocking of EpAb3-5, MJ-37 and HO-3 with VU1D-9. Fresh SKBR-3 cells were first incubated with one of the anti-EpCAM antibodies and subsequently with VU1D-9-PE.

EpAb3-5 abrogated the VU1D-9-PE signal, whereas HO-3 and MJ-37 did not. These results indicate that EpAb3-5 cross blocks with VU1D-9 (Figure 5, right column), whereas HO-3 and MJ-37 bind to different epitopes than VU1D-9 does. Control samples, where SKBR-3 cells were incubated with one

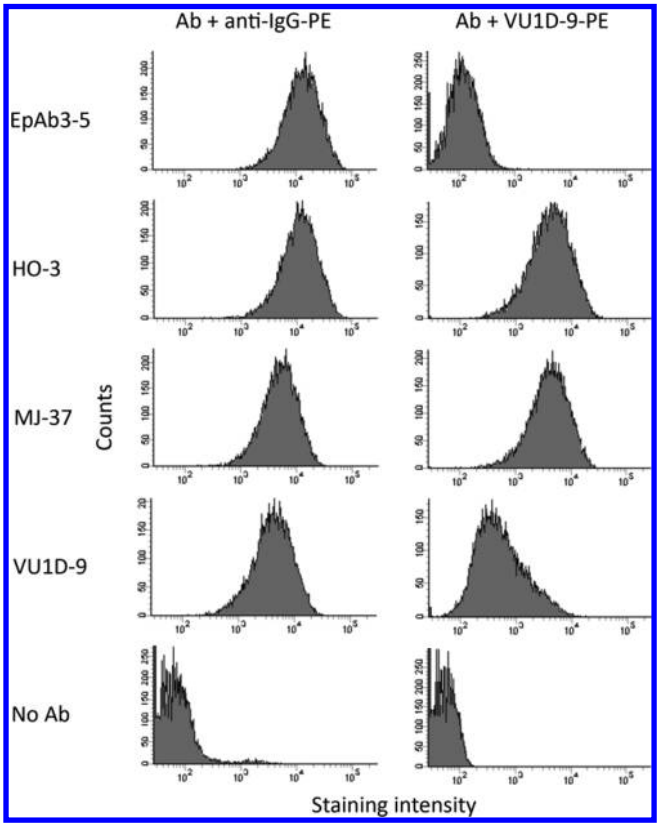

Figure 5. Determination of EpAb3-5, HO-3, and MJ-37 epitope cross blocking with VU1D-9. VU1D-9 signal is abrogated by binding of EpAb3-5 but not in the cases of HO-3 and MJ-37, indicating that the latter binds to different epitopes than VU1D-9 does.

of the anti-EpCAM antibodies and subsequently with IgG-PE, presented in Figure 5 (left columns) show normal binding of EpAb3-5, HO-3, MJ-37, and VU1D-9 to SKBR-3 cells. The bottom row shows SKBR-3 without Ab unstained (right) and the isotype control with only IgG-PE (left).

SPRi was performed to compare the binding affinity of the 4 different antibodies. Recombinant human EpCAM as well the 4 different anti-EpCAM antibodies were immobilized on the surface of a gold SPR sensor and the 4 different anti-EpCAM antibodies were injected in the system in concentrations of 32, 16, 8, 4, 2, 1, and 0.5 nM, to obtain kinetic data. The sensorgrams obtained from the measurements were used to determine the affinities and kinetics of the antibodies tested. The on-rate (k_d) and off-rate (k_a) and dissociation equilibrium (K_D) constants for various ligand densities and analyte concentrations were exponentially interpolated to the K_D at R_{max} =100. K_D represents the analyte concentration under equilibrium conditions at which 50% of the ligand molecules are bound.[28] Results are shown in Table 2. Judging by the

Table 2. Surface Plasmon Resonance Measurements of Anti-EpCAM/rhEpCAM binding

antibody	k_a (S^{-1} M^{-1})	k_d (S^{-1})	K_D (M) (R_{max} = 100)
EpAb3-5	3.1×10^{05}	1.1×10^{-05}	2.6×10^{-11}
HO-3	1.5×10^{05}	5.9×10^{-05}	4.0×10^{-11}
MJ-37	1.6×10^{05}	4.3×10^{-04}	2.8×10^{-09}
VU1D-9	3.1×10^{05}	8.2×10^{-05}	2.7×10^{-10}

determined K_D values, EpAb3-5 showed the highest binding affinity ($K_D = 2.6 \times 10^{-11}$ M) comparable to the affinity of HO-3 ($K_D = 4.0 \times 10^{-11}$ M) followed by VU1D-9 ($K_D = 2.7 \times 10^{-10}$ M) and MJ-37 respectively ($K_D = 2.8 \times 10^{-9}$ M).

SKBR-3 Capture Using Different Abs. After analyzing binding affinity and crossblocking, the antibodies were tested for the capture of EpCAM expressing cells. Moreover, the amount of captured SKBR-3 cells was expected to correlate with the obtained K_D values, i.e. more cells captured by antibodies with higher K_D values. Therefore, SKBR-3 capture was tested under flow in microscope glass slides functionalized with either EpAb3-5, HO-3, MJ-37, or VU1D-9. After functionalization, the slides were placed onto the slide channels with a height of 400 μm and 200 000 Cell Tracker Orange stained SKBR-3 cells were pipetted into the slide channel and left to incubate for 30 min. Afterward, PBS was pumped using the setup described in Scheme 2 through the channel for 30 min at 500 μL/min.

In Figure 6, each row represents the entire scanned channel, before (A) and after (B) pumping the PBS. The left surface of all slides was treated with BSA and the right side with an anti-EpCAM antibody. It is notorious, for all tested antibodies, that the amount of cells on the left side of the channel is dramatically reduced after pumping PBS, whereas the antibodies on the right side retain most of the SKBR-3 initially scanned. The BSA coated surface was used to correct for variation in coating efficiency and cell seeding between experimental days. Figure 7 shows the quantified results for these capture experiments. The total number of bound cells present in the slide after rinsing (B rows in Figure 6) was set to 100% and the diagram shows the percentage of cells present on the EpCAM functionalized surface and the percentage of cells on the BSA functionalized control surface. Comparison with the control BSA-functionalized surface showed that the HO-3

DOI: 10.1021/acsami.6b01241
ACS Appl. Mater. Interfaces 2016, 8, 14349–14356

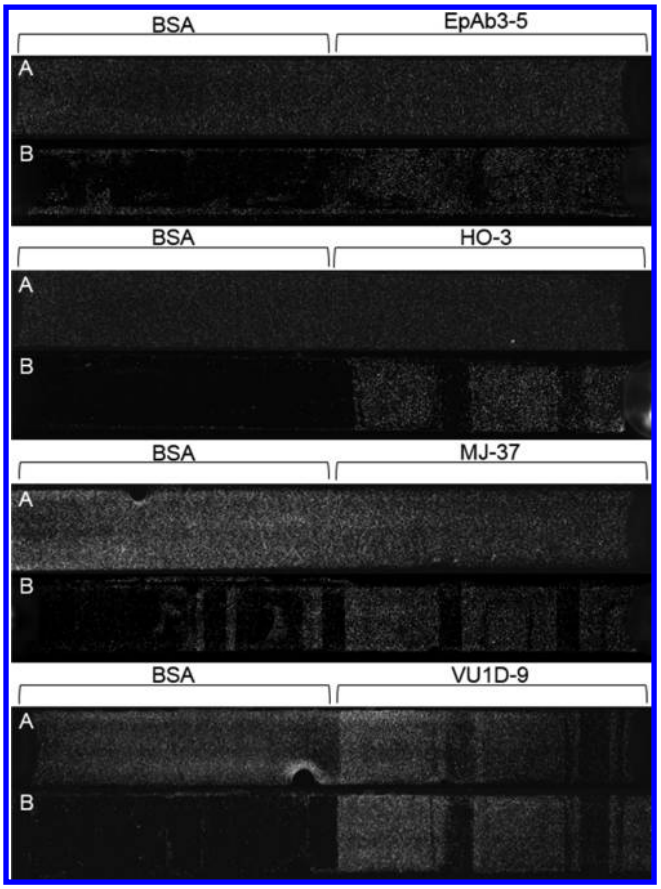

Figure 6. Determination of EpAb3-5, HO-3, MJ-37, and VU1D-9 binding of SKBR-3 under dynamic conditions. (A) Slide after cell sedimentation, (B) slide after washing by flowing the PBS.

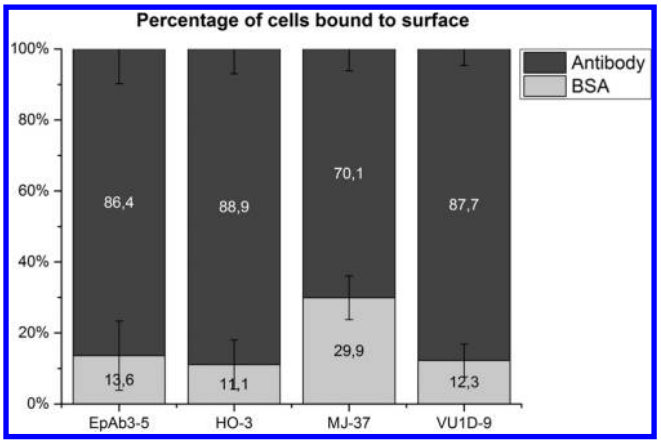

Figure 7. Quantification of bound SKBR3 cells to BSA and various anti-EpCAM antibodies functionalized surfaces under dynamic conditions. Total number of cells present on both BSA and EpCAM functionalized surface is set as 100%. (n = 3*total of 3 wells).

antibody functionalized surface bound most SKBR-3 cells (88.9% versus 11.1% with a SD of ±7.0), followed by VU1D-9 (88% versus 12% ± 4.6), EpAb3-5 (86,4% versus 13.6% ± 9.8%), and MJ-37 (70% versus 30% ± 6.1). There is a significant difference between the 4 antibodies (p = 0.037). When performing posthoc multiple comparison it shows that there is no significant difference between HO-3, EpAb3-5, and VU1D9, but there is significant difference at the 0.05 level between HO-3 and MJ-37.

DISCUSSION

Presence of CTC is associated with poor outcome and changes in the CTC count can be used to monitor treatment in cancer patients. Moreover assessment of treatment targets on CTC can guide the choice of the most effective therapy. Current techniques to isolate CTC are frequently based on immuno-based cell capture, mostly using avidin−biotin chemistry. Although the epitope target is in most cases justified, the rational for the choice of the antibody clone is often missing, which can have implications in the performance of the developed systems.

Here we present a coating that enables covalent binding of antibodies that can be used for CTC capturing. In addition we compare four different antibodies recognizing the EpCAM antigen. The choice for a PAA coating was made because a direct covalent binding of antibody on PAA is a more simple chemistry compared to the mostly used avidin−biotin chemistry. Only one activating step with well-known EDC/NHS mixture is needed while avidin−biotin chemistry consists of three steps (attachment of avidin onto surfaces, biotinylation of the antibody and coupling of biotinylated-antibody onto the avidin-coated surface). Especially, by using a polycarboxylate coating, which binds antibodies electrostatically by choosing the right pH above the pI of the antibody. A subsequent rapid reaction of NHS moieties to lysine groups available around the antibody makes the binding efficient. Because of hydrophilicity and the negative charge of the PAA layer, it also can act as a kind of hydrogel layer and plays a role as a repellent to other components. In contrast to the avidin−biotin chemistry, which is also known to have a high nonspecific binding because of its tendency to bind to other components than biotin and the strong positive charge on the avidin may cause ionic interaction, especially with cell surfaces.[29] In the case of direct binding of antibody to a PAA layer, nonspecific binding is reduced and the unreacted NHS moieties can be converted back to carboxylic acid.[30]

Functionalization of this coating with a CD3 monoclonal antibody recognizing T-lymphocytes provided the proof of concept of its binding ability by retaining lymphocytes on a CD3-coated surface, whereas the BSA-coated surface remained empty (Figure 1). BSA is inert and binds to "sticky" surface spots, thus preventing undesired binding of functional proteins.[31] Further on, we functionalized this coating with anti-EpCAM antibodies derived from the VU1D-9 clone and performed similar experiments to that of CD3. High EpCAM expressing SKBR-3 cells were retained two times more on a VU1D-9 functionalized surface as compared to a BSA-functionalized surface (Figure 2 and Table 1), further demonstrating the binding properties of the functionalized coating. Unlike in the CD3 experiment, SKBR-3 did stick to the BSA-treated surface likely due to its adhesion properties, in contrast to lymphocytes that are nonadherent cells. It is likely that in the specific case of SKBR-3 cells the incubation time was long enough to permit the assembly of focal adhesions with the surface anchoring points. This hypothesis is further strengthened by the fact that in the dynamic experiments the percentage of bound SKBR-3 cells to the VU1D-9 surface is higher (between 75 and 85%) than in the static experiment (Table 1). This indicates that the PBS flow detaches some of the already adhering SKBR-3 cells, at least those with the weakest adhesion points, thereby increasing the difference between the two conditions. More importantly, it also indicates

DOI: 10.1021/acsami.6b01241
ACS Appl. Mater. Interfaces 2016, 8, 14349−14356

that the binding affinity of the VU1D-9 antibody is sufficiently high to sustain the cell capture under flow conditions.

After showing the cell capture ability of VU1D-9-functionalized PAA coating under static conditions and dynamic washing conditions using flow, we compared the performance of other anti-EpCAM clones in our system. First, it was proven that all antibodies tested could be functionalized and detected on the coated surface (Figure 4), and second, the epitope binding and binding affinity was compared by flow cytometry. The EpAb3-5 shares the same target epitope as VU1D-9, whereas HO-3 and MJ-37 have a different epitope (Figure 5). The availability of antibodies targeting two different epitopes of the EpCAM antigens can be exploited either by increasing the binding efficiency of EpCAM bearing cells by the use of two antibodies or by using one antibody to capture the cells and another one to discriminate between the specifically and nonspecifically bound cells. In the latter case, the antibody can for example be conjugated to a fluorescent molecule and the cells examined by fluorescent microscopy.

Assessment of the affinity of the antibodies to recombinant EpCAM was done by SPRi and showed the highest binding affinity for EpAb3-5 followed by HO-3, VU1D-9, and MJ37, respectively (Table 2). Following the setup presented in Scheme 2, all antibodies were tested for their ability to capture SKBR-3 cells. The three antibodies with the highest affinity did not show a capture efficiency significantly different from each other. However, the MJ-37 antibody with the lowest affinity captured significantly less SKBR-3 cells (70%) as compared to the HO-3 antibody.

These results emphasize the need that when choosing an antibody for such applications thorough tests should be performed to make the best choice for the desired application. Evaluating binding affinity constants might anticipate the antibody performance results (as in the case of HO-3) but might not be enough and therefore other tests should be performed and taken into account before a decision is made.

CONCLUSION

We showed a simple poly(acrylic acid) coating on glass slides. Using this coating we were able to functionally bind anti-CD3 and four different types of anti-EpCAM antibodies, confirmed by lymphocyte and SKBR-3 cell binding respectively, in contrast to their BSA control surfaces where no or less cells were found. Among the four different anti-EpCAM antibodies EpAb3-5 and VU1D-9 shared the same epitope target. EpAb3-5 displayed the highest binding affinity constant when analyzed by SPRi using rhEpCAM, followed by HO-3, VU1D-9, and MJ-37 respectively. In line with the expectations, EpAb3-5, HO-3, and VU1D-9 bound most SKBR-3 cells in a flow model chamber and MJ-37 bound the least cells. These results point toward careful selection of antibody clones when targeting specific cell surface markers and emphasize the need to perform multiple assays before choosing one.

ASSOCIATED CONTENT

Supporting Information

The Supporting Information is available free of charge on the ACS Publications website at DOI: 10.1021/acsami.6b01241.

Figure S1, wide-scan XPS spectra of PAA-coated glass slide; Figure S2, narrow-scan XPS spectra of carbon region of PAA-coated glass slide (PDF)

AUTHOR INFORMATION

Corresponding Author

*E-mail: k.c.andree@utwente.nl. Telephone: +31 53 489 4187.

Present Address

⊥Stem Cell and Drug Screening Group, Center for Neuroscience and Cell Biology, Cantanhede, Portugal.

Author Contributions

‡These authors contributed equally. The manuscript was written through contributions of all authors. All authors have given approval to the final version of the manuscript.

Funding

EU FP7 HEALTH.2012.1.2-1 Project #305341 "Circulating Tumor Cells TheRapeutic Apheresis (CTCTrap): a novel biotechnology enabling personalized therapy for all cancer patients". NanoNextNL, a micro and nanotechnology consortium of the Government of The Netherlands and 130 partners. STW project #11260 Cellspread and EU IMI project # 115749-1 CANCER-ID.

Notes

The authors declare no competing financial interest.

ACKNOWLEDGMENTS

The main work is supported by EUFP7 project #305341 CTCTrap and this work is supported by NanoNextNL, a micro and nanotechnology consortium of the Government of The Netherlands and 130 partners. The positions of K.A., A.B., and J.v.D. are supported by EUFP7 project #305341 CTCTrap. The position of I.S. is supported by STW project #11260 Cellspread. The position of A.M. is supported by EU IMI project # 115749-1 CANCER-ID. The authors thank Niels van der Velde and Dr. Richard Schasfoort from IBIS Technologies B.V. for their excellent support in obtaining and analyzing the SPRi data.

ABBREVIATIONS

BSA, bovine serum albumin
CTC, circulating tumor cell
EpCAM, epithelial cell adhesion molecule
EDC, N-(3-(dimethylamino)propyl)-N′-ethylcarbodiimide hydrochloride
NHS, *N*-hydroxy-succinimide
PAA, poly(acrylic acid)
PE, phycoerythrin
pI, isoelectric point
SPRi, surface plasmon resonance imaging
XPS, X-ray photoelectron spectroscopy

REFERENCES

(1) Barradas, A. M. C.; Terstappen, L. W. M. M. Towards the Biological Understanding of CTC: Capture Technologies, Definitions and Potential to Create Metastasis. *Cancers* **2013**, *5*, 1619−1642.

(2) Alix-Panabières, C.; Pantel, K. Circulating Tumor Cells: Liquid Biopsy of Cancer. *Clin. Chem.* **2013**, *59*, 110−118.

(3) Andree, K. C.; van Dalum, G.; Terstappen, L. W. M. M. Challenges in Circulating Tumor Cell Detection by the CellSearch System. *Mol. Oncol.* **2016**, *10*, 395−407.

(4) Rao, C. G.; Chianese, D.; Doyle, G. V.; Miller, M. C.; Russell, T.; Sanders, R. A.; Terstappen, L. W. M. M. Expression of Epithelial Cell Adhesion Molecule in Carcinoma Cells Present in Blood and Primary and Metastatic Tumors. *Int. J. Oncol.* **2005**, *27*, 49−57.

(5) Schnell, U.; Cirulli, V.; Giepmans, B. N. G. EpCAM: Structure and Function in Health and Disease. *Biochim. Biophys. Acta, Biomembr.* **2013**, *1828*, 1989−2001.

DOI: 10.1021/acsami.6b01241
ACS Appl. Mater. Interfaces 2016, 8, 14349−14356

(6) Koprowski, H.; Steplewski, Z.; Mitchell, K.; Herlyn, M.; Herlyn, D.; Fuhrer, P. Colorectal Carcinoma Antigens Detected by Hybridoma Antibodies. *Somatic Cell Genet.* **1979**, *5*, 957−971.
(7) Patriarca, C.; Macchi, R. M.; Marschner, A. K.; Mellstedt, H. Epithelial Cell Adhesion Molecule Expression (CD326) in Cancer: A Short Review. *Cancer Treat. Rev.* **2012**, *38*, 68−75.
(8) Flatmark, K.; Borgen, E.; Nesland, J. M.; Rasmussen, H.; Johannessen, H.-O.; Bukholm, I.; Rosales, R.; Hårklau, L.; Jacobsen, H. J.; Sandstad, B.; Boye, K.; Fodstad, Ø. Disseminated Tumour Cells as a Prognostic Biomarker in Colorectal Cancer. *Br. J. Cancer* **2011**, *104*, 1434−1439.
(9) Osta, W. A.; Chen, Y.; Mikhitarian, K.; Mitas, M.; Salem, M.; Hannun, Y. A.; Cole, D. J.; Gillanders, W. E. EpCAM Is Overexpressed in Breast Cancer and Is a Potential Target for Breast Cancer Gene Therapy. *Cancer Res.* **2004**, *64*, 5818−5824.
(10) Imano, M.; Itoh, T.; Satou, T.; Yasuda, A.; Nishiki, K.; Kato, H.; Shiraishi, O.; Peng, Y.-F.; Shinkai, M.; Tsubaki, M.; Yasuda, T.; Imamoto, H.; Nishida, S.; Takeyama, Y.; Furkawa, H.; Okuno, K.; Shiozaki, H. High Expression of Epithelial Cellular Adhesion Molecule in Peritoneal Metastasis of Gastric Cancer. *Target. Oncol.* **2013**, *8*, 231−235.
(11) Ni, J.; Cozzi, P. J.; Duan, W.; Shigdar, S.; Graham, P. H.; John, K. H.; Li, Y. Role of the EpCAM (CD326) in Prostate Cancer Metastasis and Progression. *Cancer Metastasis Rev.* **2012**, *31*, 779−791.
(12) Ji, J.; Yamashita, T.; Budhu, A.; Forgues, M.; Jia, H.-L.; Li, C.; Deng, C.; Wauthier, E.; Reid, L. M.; Ye, Q.-H.; Qin, L.-X.; Yang, W.; Wang, H.-Y.; Tang, Z.-Y.; Croce, C. M.; Wang, X. W. Identification of microRNA-181 by Genome-Wide Screening as a Critical Player in EpCAM-Positive Hepatic Cancer Stem Cells. *Hepatology* **2009**, *50*, 472−480.
(13) Simon, M.; Stefan, N.; Plückthun, A.; Zangemeister-Wittke, U. Epithelial Cell Adhesion Molecule-Targeted Drug Delivery for Cancer Therapy. *Expert Opin. Drug Delivery* **2013**, *10*, 451−468.
(14) Cristofanilli, M.; Budd, G. T.; Ellis, M. J.; Stopeck, A.; Matera, J.; Miller, M. C.; Reuben, J. M.; Doyle, G. V.; Allard, W. J.; Terstappen, L. W. M. M.; Hayes, D. F. Circulating Tumor Cells, Disease Progression, and Survival in Metastatic Breast Cancer. *N. Engl. J. Med.* **2004**, *351*, 781−791.
(15) Ozkumur, E.; Shah, A. M.; Ciciliano, J. C.; Emmink, B. L.; Miyamoto, D. T.; Brachtel, E.; Yu, M.; Chen, P.; Morgan, B.; Trautwein, J.; Kimura, A.; Sengupta, S.; Stott, S. L.; Karabacak, N. M.; Barber, T. A.; Walsh, J. R.; Smith, K.; Spuhler, P. S.; Sullivan, J. P.; Lee, R. J.; Ting, D. T.; Luo, X.; Shaw, A. T.; Bardia, A.; Sequist, L. V.; Louis, D. N.; Maheswaran, S.; Kapur, R.; Haber, D. A.; Toner, M. Inertial Focusing for Tumor Antigen-Dependent and -Independent Sorting of Rare Circulating Tumor Cells. *Sci. Transl. Med.* **2013**, *5*, 179ra47.
(16) Kirby, B. J.; Jodari, M.; Loftus, M. S.; Gakhar, G.; Pratt, E. D.; Chanel-Vos, C.; Gleghorn, J. P.; Santana, S. M.; Liu, H.; Smith, J. P.; Navarro, V. N.; Tagawa, S. T.; Bander, N. H.; Nanus, D. M.; Giannakakou, P. Functional Characterization of Circulating Tumor Cells with a Prostate-Cancer-Specific Microfluidic Device. *PLoS One* **2012**, *7*, e35976.
(17) Nagrath, S.; Sequist, L. V.; Maheswaran, S.; Bell, D. W.; Irimia, D.; Ulkus, L.; Smith, M. R.; Kwak, E. L.; Digumarthy, S.; Muzikansky, A.; Ryan, P.; Balis, U. J.; Tompkins, R. G.; Haber, D. A.; Toner, M. Isolation of Rare Circulating Tumour Cells in Cancer Patients by Microchip Technology. *Nature* **2007**, *450*, 1235−1239.
(18) Stott, S. L.; Hsu, C.-H.; Tsukrov, D. I.; Yu, M.; Miyamoto, D. T.; Waltman, B. A.; Rothenberg, S. M.; Shah, A. M.; Smas, M. E.; Korir, G. K.; Floyd, F. P.; Gilman, A. J.; Lord, J. B.; Winokur, D.; Springer, S.; Irimia, D.; Nagrath, S.; Sequist, L. V.; Lee, R. J.; Isselbacher, K. J.; Maheswaran, S.; Haber, D. A.; Toner, M. Isolation of Circulating Tumor Cells Using a Microvortex-Generating Herringbone-Chip. *Proc. Natl. Acad. Sci. U. S. A.* **2010**, *107*, 18392−18397.
(19) Liao, M.-Y.; Lai, J.-K.; Kuo, M. Y.-P.; Lu, R.-M.; Lin, C.-W.; Cheng, P.-C.; Liang, K.-H.; Wu, H.-C. An Anti-EpCAM Antibody EpAb2−6 for the Treatment of Colon Cancer. *Oncotarget* **2015**, *6*, 24947−24968.
(20) Ruf, P.; Gires, O.; Jäger, M.; Fellinger, K.; Atz, J.; Lindhofer, H. Characterisation of the New EpCAM-Specific Antibody HO-3: Implications for Trifunctional Antibody Immunotherapy of Cancer. *Br. J. Cancer* **2007**, *97*, 315−321.
(21) De Leij, L.; Helrich, W.; Stein, R.; Mattes, M. J. SCLC-Cluster-2 Antibodies Detect the Pancarcinoma/epithelial Glycoprotein EGP-2. *Int. J. Cancer* **1994**, *57* (S8), 60−63.
(22) Natarajan, S.; Katsamba, P. S.; Miles, A.; Eckman, J.; Papalia, G. A.; Rich, R. L.; Gale, B. K.; Myszka, D. G. Continuous-Flow Microfluidic Printing of Proteins for Array-Based Applications Including Surface Plasmon Resonance Imaging. *Anal. Biochem.* **2008**, *373*, 141−146.
(23) Schasfoort, R. B. M.; Andree, K. C.; van der Velde, N.; van der Kooi, A.; Stojanović, I.; Terstappen, L. W. M. M. Interpolation Method for Accurate Affinity Ranking of Arrayed Ligand-Analyte Interactions. *Anal. Biochem.* **2016**, *500*, 21−23.
(24) Preibisch, S.; Saalfeld, S.; Tomancak, P. Globally Optimal Stitching of Tiled 3D Microscopic Image Acquisitions. *Bioinformatics* **2009**, *25*, 1463−1465.
(25) Vermette, P.; Meagher, L. Immobilization and Characterization of Poly(acrylic Acid) Graft Layers. *Langmuir* **2002**, *18*, 10137−10145.
(26) Louette, P.; Bodino, F.; Pireaux, J.-J. Poly(acrylic Acid) (PAA) XPS Reference Core Level and Energy Loss Spectra. *Surf. Sci. Spectra* **2005**, *12*, 22.
(27) Tsubura, A.; Senzaki, H.; Sasaki, M.; Hilgers, J.; Morii, S. Immunohistochemical Demonstration of Breast-Derived And/or Carcinoma-Associated Glycoproteins in Normal Skin Appendages and Their Tumors. *J. Cutaneous Pathol.* **1992**, *19*, 73−79.
(28) Schasfoort, R. B. M.; de Lau, W.; van der Kooi, A.; Clevers, H.; Engbers, G. H. M. Method for Estimating the Single Molecular Affinity. *Anal. Biochem.* **2012**, *421*, 794−796.
(29) Hermanson, G. T. *Bioconjugate Techniques*, third ed.; Academic Press: Boston, 2013.
(30) Vermette, P.; Gengenbach, T.; Divisekera, U.; Kambouris, P. A.; Griesser, H. J.; Meagher, L. Immobilization and Surface Characterization of NeutrAvidin Biotin-Binding Protein on Different Hydrogel Interlayers. *J. Colloid Interface Sci.* **2003**, *259*, 13−26.
(31) Sperling, R. A.; Parak, W. J. Surface Modification, Functionalization and Bioconjugation of Colloidal Inorganic Nanoparticles. *Philos. Trans. R. Soc., A* **2010**, *368*, 1333−1383.

DOI: 10.1021/acsami.6b01241
ACS Appl. Mater. Interfaces 2016, 8, 14349−14356